23rd AIAA Applied Aerodynamics Conference
6 - 9 June 2005, Toronto, Ontario Canada

AIAA 2005-4971

A Cambered Body Method for Missile Datcom

William B. Blake *
Air Force Research Laboratory, Wright Patterson AFB OH 45433

Etan D. Karni #
Purdue University, West Lafayette IN 47907

A method for analyzing cambered bodies has been incorporated into Missile Datcom. Existing methods based on mean line theory, slender body theory, viscous crossflow theory were assessed. They were compared with wind tunnel data from subsonic to supersonic speeds for cambered bodies with axi-symmetric cross-sections. The comparison cases consisted of three configurations with discrete camber changes (deflectable nose missile) and twelve configurations with continuous camber changes. A combination of slender body and viscous crossflow theory was found to provide the best agreement with experimental data.

Nomenclature

C_{mac} = Pitching moment coefficient at zero lift
C_{mo} = Pitching moment coefficient at zero angle of attack
C_{No} = Normal force coefficient at zero angle of attack
C_p = Pressure coefficient
l = Body length
l_{ref} = Reference length for pitching moment
S_{ref} = Reference area
S_{plan} = Body planform area
R = Body radius
U = Freestream Velocity
x = Longitudinal position of body mean line
x_{ref} = Longitudinal position of moment reference center
z = Vertical position of body mean line
α_{0L} = Angle of attack for zero lift
ϕ = Velocity potential

I Introduction

Missile Datcom[1] is a widely used engineering-level code that uses the component buildup technique to predict vehicle aerodynamics. Both theoretical and empirical methods are included that encompass the entire speed regime from subsonic to hypersonic. The program has been shown to provide excellent agreement with experimental data for a variety of configurations[2,3]. From the initial 11/85 version of the code to the 9/02 release, only uncambered bodies of circular or elliptic cross-section could be defined. The code is currently being applied to various types of re-entry vehicles[4], many of which have significant nose camber for thermal protection. To provide improved results for these types of configurations, a cambered body method has been incorporated into the code. Deflectable noses have also been studied as pitch control devices for conventional missiles[5], and a cambered body method would allow for evaluation of these configurations as well. Two existing cambered body methods were compared. The first, from mean line theory[6], was found to provide mixed agreement compared to test data. The second, from on slender body theory[7], provided better agreement with data but accuracy was degraded for bodies with discrete camber changes. Adding an increment for the viscous crossflow contribution improved the results for these bodies.

II Methods Assessed

*Aerospace Engineer, Air Vehicles Directorate, 2210 Eighth St, Associate Fellow AIAA
Senior, Department of Aerospace Engineering, Student Member AIAA

Mean Line Theory

The first method examined is taken from the Digital Datcom computer program. Digital Datcom uses a method adapted from thin airfoil theory to compute the angle of attack for zero lift and zero lift pitching moment for a cambered body. This method is based on the shape of the mean line only, and is independent of the cross-sectional area distribution of the body. The equations, as given in the Program Implementation Guide[6], are:

$$\alpha_{0L} = \int_0^{0.95} \frac{-(z/l)d(x/l)}{\pi(1-x/l)\sqrt{x/l-(x/l)^2}} \qquad [1]$$

$$C_{mac} = \left[2\int_0^{0.95} \frac{(z/l)(1-2x/l)d(x/l)}{\sqrt{x/l-(x/l)^2}} \right] \frac{S_{plan}}{S_{ref}} \frac{l}{l_{ref}} \qquad [2]$$

Initial application of these equations gave extremely poor results, so their origin was investigated. Mean line theory assumes that the leading and trailing edges are connected by a straight line (the "chord" line), and that the camber variation, z(x), is the deviation of the actual shape from that line. This makes z(0)=z(l)=0 and places the reference line at zero angle of attack. As coded in Digital Datcom, no adjustment is made to camber lines that do not satisfy the z(0)=z(l)=0 condition. The method was revised to rotate the user input to match this condition, and then subtract the resulting incidence from the final result. In addition, the pitching moment equation differs from that given by thin airfoil theory in several respects. The result given by Keuthe and Schetzer[8] is:

$$C_{mac} = \frac{\pi}{2}\alpha_{0L} + 2\int_0^1 \frac{(z/l)(1-2x/l)d(x/l)}{\sqrt{x/l-(x/l)^2}} \qquad [3]$$

The Digital Datcom result includes a correction term for the reference area and length, and neglects the zero lift angle of attack term. It gave extremely large pitching moments that were presumed to come from the reference area correction, the justification of which is unknown. The pitching moment equation was revised to match the Keuthe and Schetzer result with only the reference length correction included. The upper limits of the integrals were set to 0.98 instead of 1 to avoid the trailing edge singularity. Results for a NACA 4412 airfoil were generated to verify the coding. The computed results for angle of attack for zero lift and zero lift pitching moment were -3.6 deg and -0.090 respectively, which compare very well with the experimental values[8] of -3.9 deg and -0.095.

Slender Body Theory

The second method examined is based on slender body theory and was taken initially from the Low Observable Design Synthesis Tool (LODST)[7]. This method was developed for arbitrary bodies and approximates the cross-section at each body station with a polygon consisting of a set of straight line segments. The method was found to give good results for configurations with smoothly varying camber but unpredictable results for bodies with abrupt slope changes or long afterbodies. The discrepancies were traced to the way the program calculates the geometry used internally from the user inputs. After numerous attempts to correct the problem were unsuccessful, a revised subroutine was written based on the slender body theory given by Liepmann and Roshko[9]. This gave either the same or better results than the LODST method and was more robust to changes in body geometry definition. The normal force of a body of revolution is given by:

$$C_N = \frac{-1}{S_{ref}} \int_0^l \int_0^{2\pi} C_p \, R\cos\theta \, d\theta \, dx \qquad [7]$$

The pressure coefficient is obtained by differentiating the velocity potential:

$$\phi = U\alpha \frac{R(x)^2}{r}\cos\theta \qquad [8]$$

$$C_p = \frac{-2}{U}\frac{\partial\phi}{\partial x} - \left(\frac{\partial R}{\partial x}\right)^2 + (1-4\sin^2\theta)\alpha^2 \qquad [9]$$

Only the first term contributes to normal force. To assess variable camber, the angle of attack is replaced by the local slope of the body camber at the mean line (ε):

$$\alpha = \alpha_o + \varepsilon(x) \quad [10]$$

$$\varepsilon = -dz/dx \quad [11]$$

This gives:

$$C_p = -4(\alpha_0 + \varepsilon)\frac{dR}{dx}\cos\theta - 2R\frac{d\varepsilon}{dx}\cos\theta \quad [12]$$

$$C_N = \frac{4\pi}{S_{ref}}\left[\alpha_o\int_0^l R\frac{dR}{dx}dx + \int_0^l \varepsilon R\frac{dR}{dx}dx + \int_0^l \frac{R^2}{2}\frac{d\varepsilon}{dx}dx\right] \quad [13]$$

The above result was also arrived at by Beane and Durgin[10]. The first integral in Eq. [13] represents the lift of an uncambered body having the same radius distribution and basic angle of attack as the cambered body, and can be evaluated directly. The second and third integrals represent the incremental lift due to camber. If the second integral is integrated by parts, one of the two resulting terms exactly cancels the third term, leaving (for a pointed body):

$$C_N = 2(\alpha_o + \varepsilon_{base})\frac{S_{base}}{S_{ref}} \quad [15]$$

This is the classic result from slender body theory that "*the force depends only on the base configuration and angle of attack and is independent of the forward shape*".[11] This means that zero normal force will result from a cambered nose with mounted on an uncambered afterbody. The pitching moment is given by:

$$C_m = \frac{4\pi}{S_{ref}l_{ref}}\left[\int_0^l (x_{ref} - x)(\alpha_o + \varepsilon)R\frac{dR}{dx}dx + \int_0^l (x_{ref} - x)\frac{R^2}{2}\frac{d\varepsilon}{dx}dx\right] \quad [14]$$

The reference angle of attack (α_o) is assumed to be zero for the present application.

Viscous Crossflow Theory

The viscous crossflow theory of Allen[12] can also be applied to cambered bodies, although its contribution is negligible unless the local body slope is significant, because the cross-force is proportional to $\sin^2(\varepsilon)$. In contrast to the slender body result, it gives a non-zero contribution for cambered configurations with an uncambered afterbody. The viscous contribution is given by:

$$C_N = \frac{\eta c_{Dc}}{S_{ref}}\int_0^l (2R)\sin^2(\alpha_o + \varepsilon)\,dx \quad [15]$$

$$C_m = \frac{\eta c_{Dc}}{S_{ref}l_{ref}}\int_0^l (x_{ref} - x)(2R)\sin^2(\alpha_o + \varepsilon)\,dx \quad [16]$$

The reference angle of attack (α_o) is assumed to be zero for the present application. The cross flow drag coefficient is a function of the cross flow Mach number, which is very small for most cambered bodies at zero angle of attack, and changes for bodies with variable camber. Given this, and the approximate nature of this theory, a value of 1.2 was assumed for the cross flow drag coefficient. The proportionality factor η is a function of both Mach number and fineness ratio and was obtained from existing Missile Datcom tables.

III Results

Comparisons between the various methods and experimental data for a variety of cambered bodies will be shown. Most of the results shown will be normal force and pitching moment at zero angle of attack. At low to moderate angles of attack, adding camber to a body typically just shifts the normal force and pitching moment curves by a constant increment. As implemented in the Missile Datcom code, only these increments are predicted, and the results are added to the Missile Datcom prediction for the basic (uncambered) body. Second order effects such as the modified forebody vortex structure are ignored.

For the majority of the cases, adding the viscous crossflow contribution to either of the potential flow methods slightly improved the results. As a result, only two sets of predictions will be shown for each configuration, a combination of mean line theory and viscous crossflow theory, which will be denoted by "MLT", and a combination of slender body theory and viscous crossflow theory, which will be denoted by "SBT".

Mean line theory provides zero lift angle of attack, not lift at zero angle of attack. Mean line theory results for normal force at zero angle of attack were computed using the slender body theory derived lift curve slope:

$$C_{N0} = -2\alpha_{0L} \qquad [17]$$

The zero lift angle of attack includes the rotation of the body back to its original orientation (from z(0)=z(l)=0). Mean line theory pitching moment at zero lift was computed using the pitching moment slope from slender body theory:

$$C_{m0} = C_{mac} - C_{m\alpha}\alpha_{0L} \qquad [18]$$

NASA TMX-56

Gapcynski[13] tested four bodies with varying types of camber at a speed of Mach 2.01. The bodies consisted of a five caliber tangent ogive nose on a cylindrical afterbody of equal length (Fig. 1). Body 2 used a deflectable nose with the nose drooped four degrees relative to the uncambered afterbody. Body 3 had a circular arc camber line with a maximum camber of 2.6% body length at the midpoint. Body 4 had the same nose camber as body 3 with the afterbody cambered upward instead of downward, with the center of the base higher than the apex by 5.2% body length. The moment reference center was at 50% of the body length, the reference length was the overall body length.

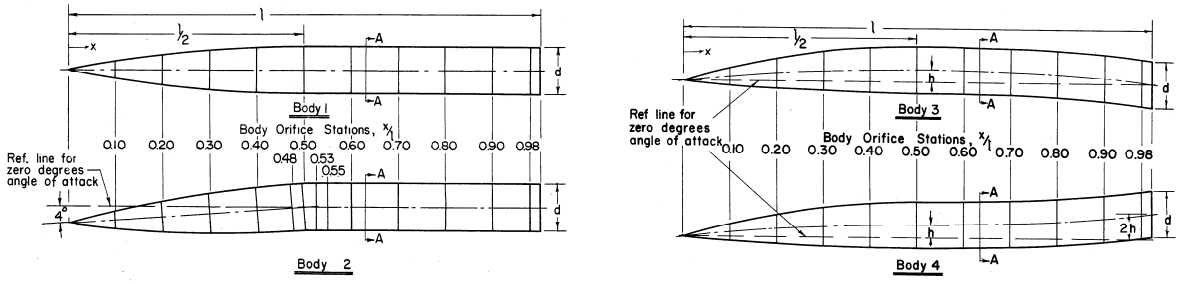

Figure 1. NASA TM X-56 Cambered Body Configurations.

Predicted values for normal force and pitching moment at zero angle of attack are compared with the test data in Figures 2 and 3. The SBT results are superior to the MLT results for all configurations for both normal force and pitching moment.

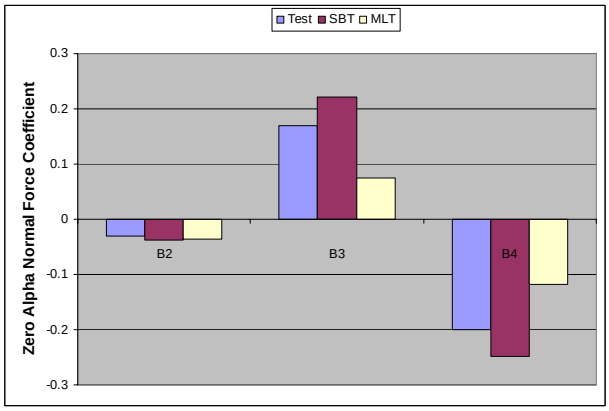

Fig 2. TMX-56 Normal Force Comparison

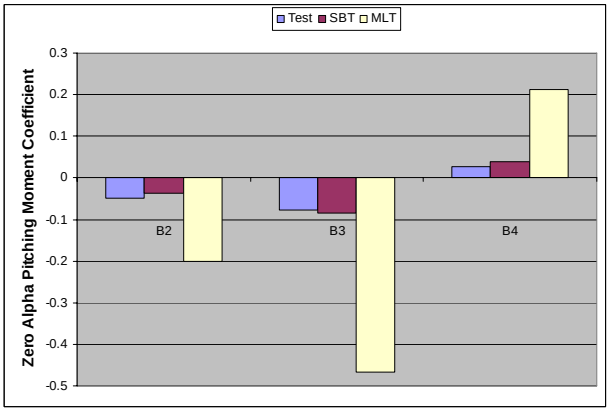

Fig 3. TMX-56 Pitching Moment Comparison

NASA TMX-270

Riley[5] gives results for a deflectable nose on a wingless missile (Figure 4) at a Mach number of 3.11. The nose consisted of a 3 caliber cone mounted on a 7 caliber cylindrical afterbody. The moment reference center was at 50% of the body length, the reference length was the body diameter. A series of tail fins and a flare were tested with and without nose deflection, and it was found that the incremental effect nose deflection was not changed by their presence.

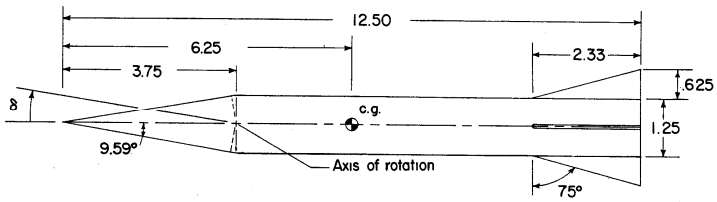

Figure 4. NASA TM X-270 Deflectable Nose Configuration.

Predicted values for normal force and pitching moment at zero angle of attack are compared with the test data in Figures 5 and 6. The data were taken from relatively small plots, the maximum accuracy is 0.05 at best for both parameters. Both methods agree with each other, and underpredict both normal force and pitching moment. Although some of the discrepancy may be due to interference between the tail and nose vortices, this cannot be the major contributor since any added force on the tail would provide a moment of the opposite sign, which is inconsistent with the error in the predictions.

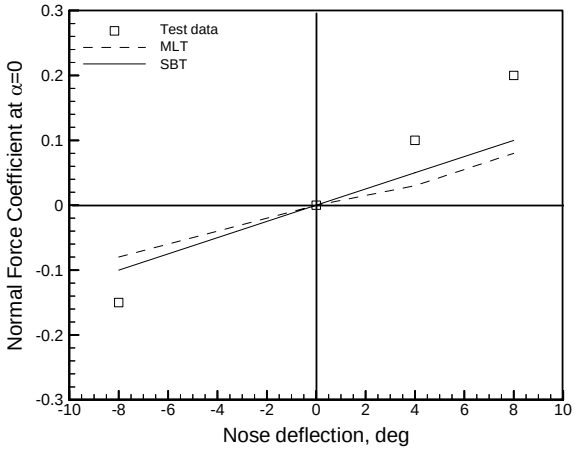

Fig 5. Effect of Nose Deflection on Normal Force, NASA TMX 270.

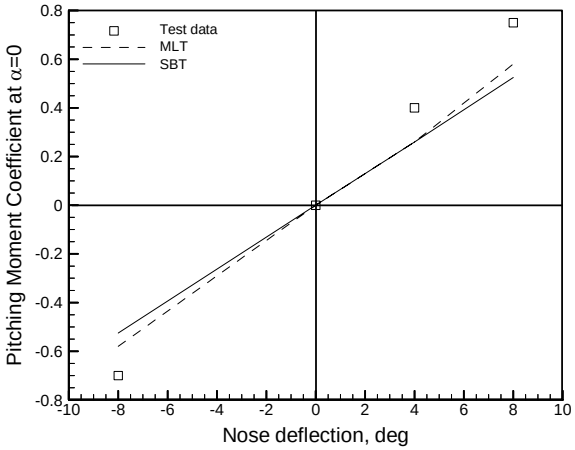

Fig 6. Effect of Nose Deflection on Pitching Moment, NASA TMX-270.

ASD TR 61-295

Beane and Durgin[10] give results for two cambered bodies that were tested in an investigation of aeroelastic effects on hypersonic stability and control. Two rigid models were constructed with camber distributions representative of bending modes of a high fineness ratio missile configuration (Figure 7). The actual deformations are much smaller than depicted in this figure. The reference body is 18 inches long with a 7.5 inch conical nose and a 1.5 inch diameter cylindrical afterbody. Forces and moments were obtained by integrating pressures that were measured at 13 stations along the body. Data for the isolated bodies without canards or wings are only given at Mach 3. The moment reference center was at the nose.

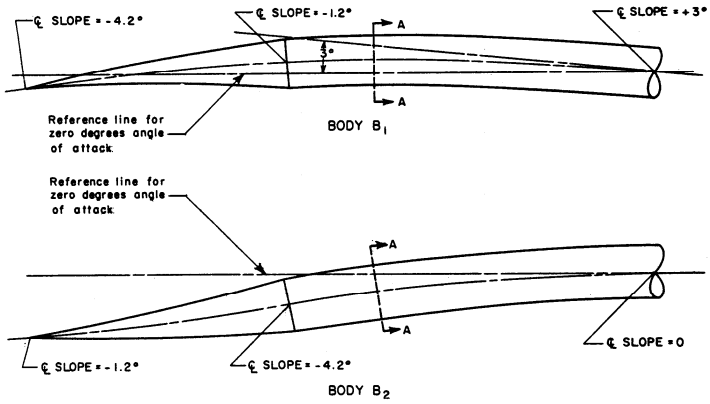

Figure 7. ASD TR 61-295 Cambered Body Configurations

Figure 8 presents the normal force distribution measured on body B1 and corresponding predictions from SBT. The individual terms in the SBT analysis are identified as dashed curves. Overall the agreement is good except for the spike at the cone-cylinder junction, 5 calibers aft of the nose. Only the nose contributes to the dR/dx term (see Eq. 13) while the entire body contributes to the dε/dx term due to the continuous curvature. In the nose region, these terms have opposing contributions and the sum is well predicted except at the juncture. Figure 9 presents a similar result for body B2. Here, the dR/dx and dε/dx terms are additive at the nose, with the dR/dx term dominating, while only the dε/dx term contributes aft of the cone-cylinder juncture. The dε/dx term reverses sign between bodies B1 and B2 due to the change from convex to concave curvature on the nose. The agreement is good everywhere except immediately aft of the juncture.

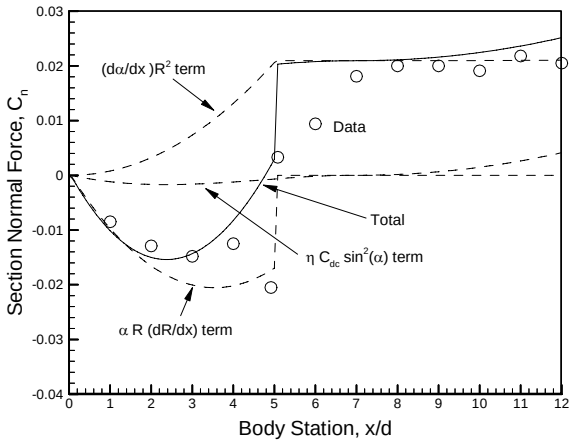

Fig 8. SBT and Measured Load Distributions Body B1, M=3

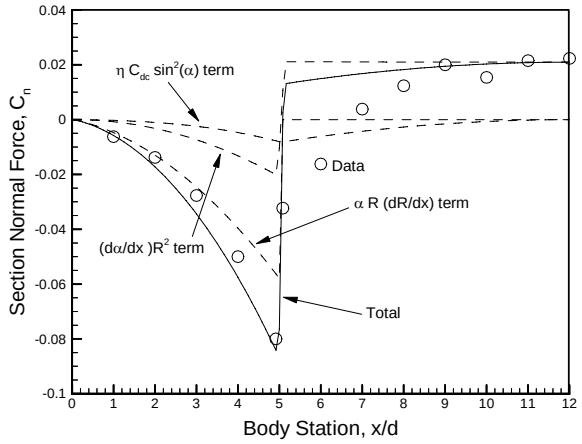

Fig 9. SBT and Measured Load Distributions Body B2, M=3.

Predicted values for normal force and pitching moment at zero angle of attack are compared with the test data in Figures 10 and 11. SBT is superior to MLT although both methods over-predict normal force for Body B2.

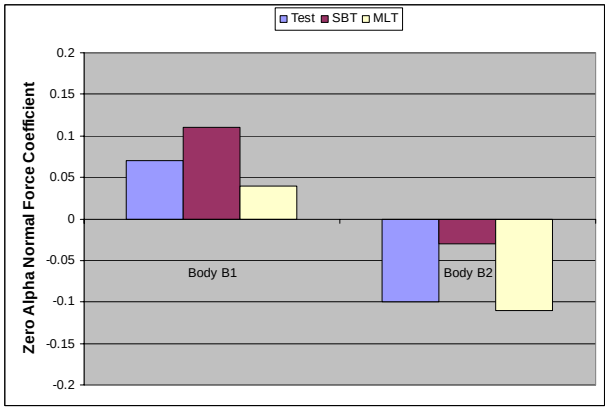

Fig 10. TR 61-295 Normal Force Comparison

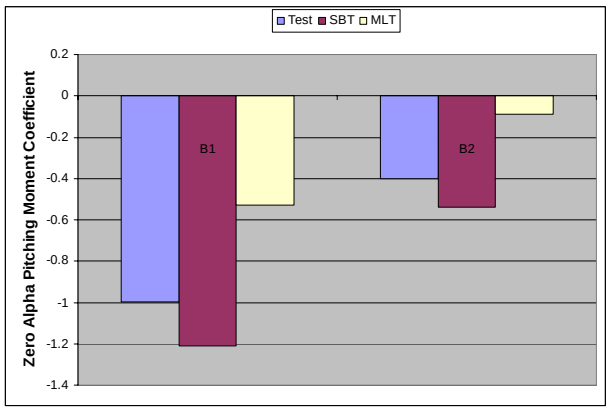

Fig 11. TR 61-295 Pitching Moment Comparison

NASA TN D-2389/TN D 2622

Spencer and Phillips[14,15] give results for a series of cambered forebodies with varying ellipticity at transonic and supersonic speeds. The upper surface of the bodies was flat with the lower surface defined by a 2/3 power law (Figure 12). Normal force and pitching moment results are presented for two nose fineness ratios, 3 and 7. Only results for the circular cross-section bodies will be presented here.

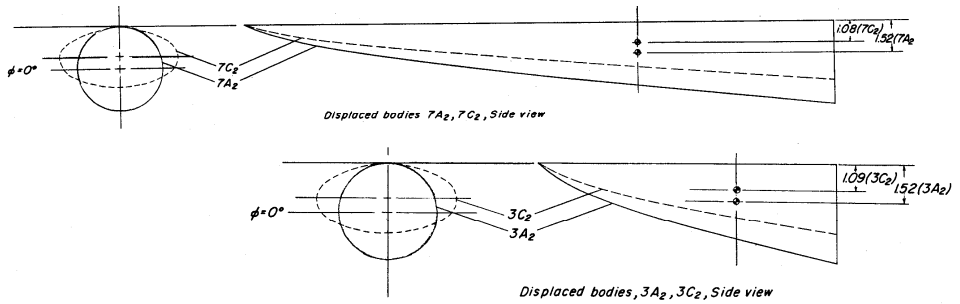

Figure 12. NASA TN D-2389/TN D-2622 Cambered Body Configuration

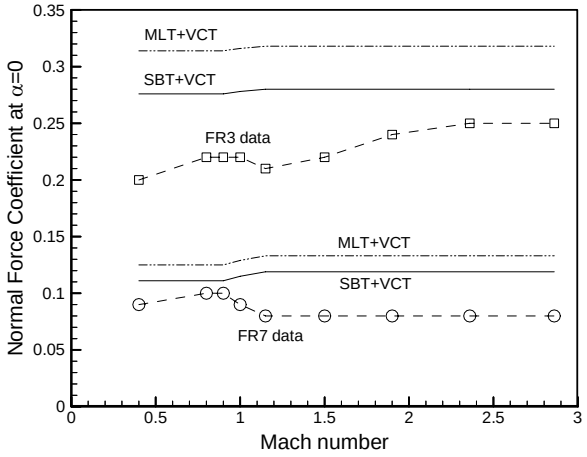

Fig. 13. Effect of Mach number on Normal Force NASA TN D-2389/2622

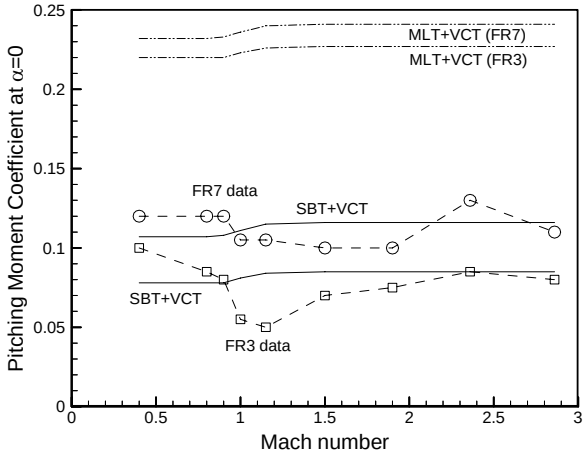

Fig. 14. Effect of Mach number on Pitching Moment NASA TN D-2389/2622

Figure 13 compares prediction with data for the normal force at zero angle of attack. The data do not vary significantly with Mach number, which both methods support. The lower fineness ratio nose has a higher effective

incidence, resulting in increased normal force at zero angle of attack. While the predictions are higher than the data for both configurations, the SBT predictions are closer to the data than the MLT predictions. Figure 14 compares the pitching moment results. Again, the data do not vary significantly with Mach number. The SBT predictions are very good in both cases, while the MLT predictions are high by a factor of two. The variation in the predicted values with Mach number arises from the viscous crossflow contribution.

NASA TP 2206

Shrout and Covell[16] give results for a series of cambered noses attached to a cylindrical afterbody (Figure 15). This was a study of the effect of nose droop on a fuselage typical of a modern fighter.

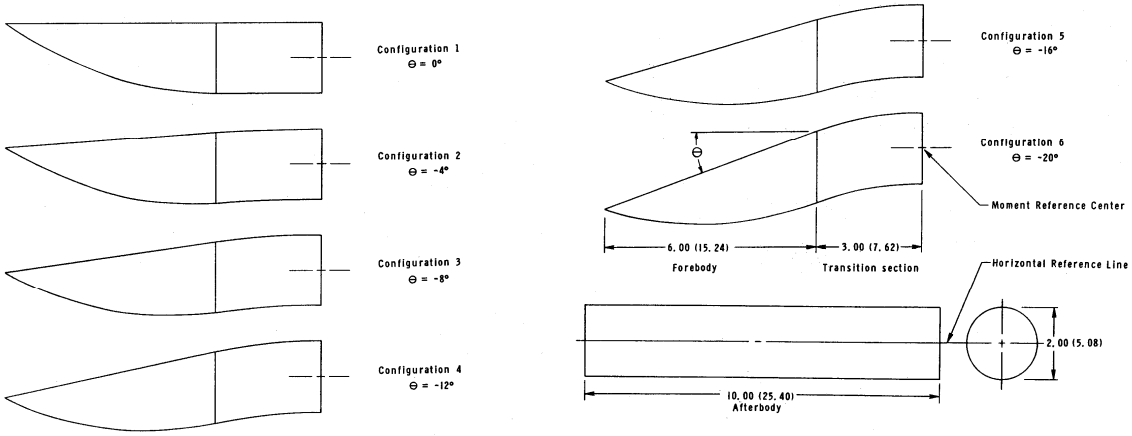

Figure 15. NASA TP 2206 Cambered Body Configurations

All noses were of the same fineness ratio and drooped in 4 degree increments from zero droop (flat upper surface) to 20 degrees downward (highly cambered). All changes in body radius and camber were continuous. Their results are plotted vs lift coefficient instead of angle of attack, and a summary plot of zero lift pitching moment vs Mach number is given in the report. The data from this plot are compared to SBT for all of the noses tested in Figures 16 and 17. Normal force results are mixed, with the data showing a much larger variation with Mach number than the prediction. The pitching moment results are very good, and except for the most highly cambered noses, the data are effectively independent of Mach number. Large losses in lift at supersonic speeds were found for Configuration 6 that the authors attributed to flow separation due to the extreme amount of droop. MLT results for these configurations were poor and are not shown.

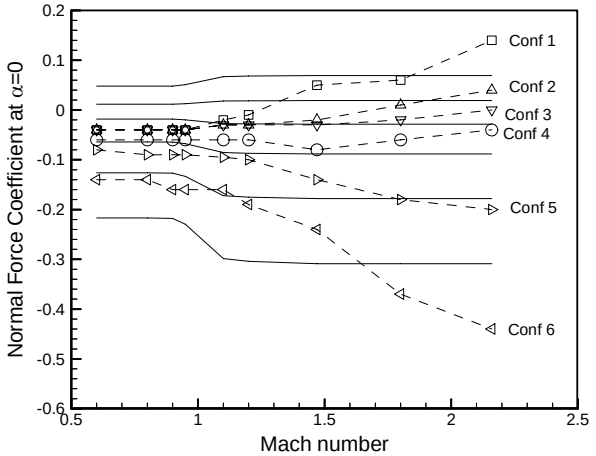

Fig. 16. Effect of Mach number on Normal Force NASA TP 2206

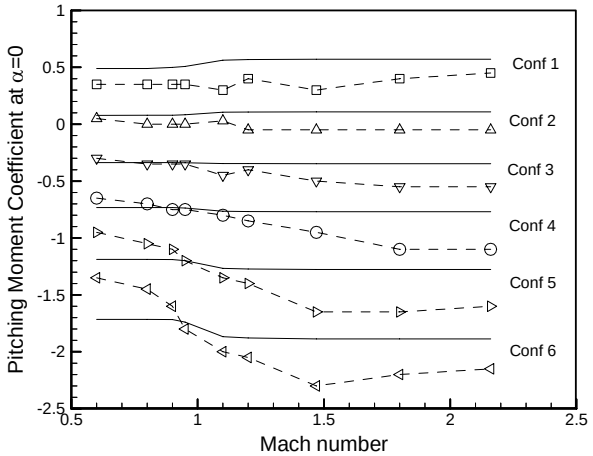

Fig. 17. Effect of Mach number on Pitching Moment NASA TP 2206

The results thus far indicate that the SBT method is superior to the MLT method, so the SBT method was incorporated into the Missile Datcom source code (Subroutine CAMBOD) and the cases were re-analyzed to verify the coding. Subroutine CAMBOD is called after the aerodynamic predictions of the basic, uncambered body have been generated, computes the incremental normal force and pitching moment due to camber, and adds the result to the uncambered case. After the code modifications were complete, the updated code was sent to the Army Aviation and Missile Command, Huntsville AL, who were undertaking a parallel effort[16] to improve the code in other areas. The Army conducted an independent test of the cambered body method using a database they had recently generated on a deflectable nose missile. The results are shown below.

AIAA 2003-3805

Landers et al[18] give results for a missile with a deflectable nose at Mach number of 3 and 6 (Figure 18). The nose was a 0.70 power law shape of fineness ratio 4. The configuration also included eight low aspect ratio tail fins, and had the moment reference center at 0.50 body length.

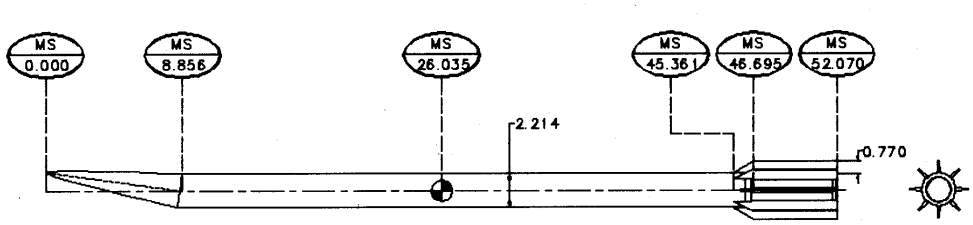

Figure 18. AIAA 2003-3805 Deflectable Nose Comparison

The predicted variation of normal force with angle of attack for zero, four and eight degrees of nose deflection is shown in Figures 19 and 20 for Mach numbers of 3 and 6. The offset due to camber at zero angle of attack is very well predicted by the code (SBT method) at both Mach numbers. At Mach 3, the code underpredicts the normal force as angle of attack increases. At Mach 6, the results are better and the data indicate the incremental effect of camber is invariant with angle of attack.

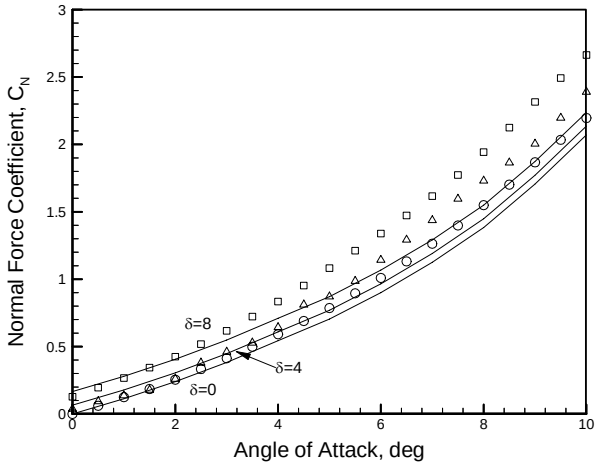

Fig. 19. Effect of Nose Deflection on Normal Force Mach=3, AIAA 2003-3805

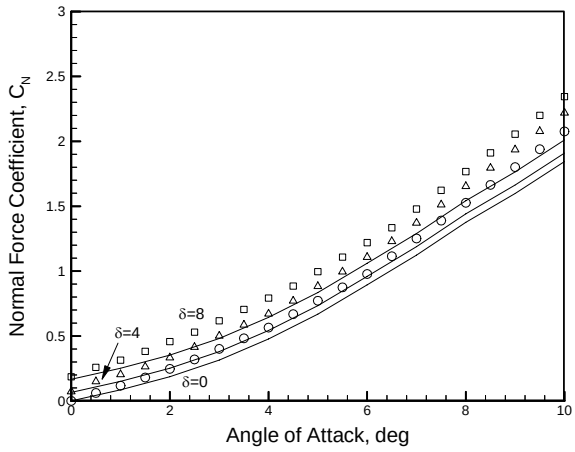

Fig. 20. Effect of Nose Deflection on Normal Force Mach=6, AIAA 2003-3805

The predicted variation of pitching moment with angle of attack for zero, four and eight degree nose deflections is shown in Figures 21 and 22 for Mach numbers of 3 and 6. The results are similar to the normal force correlations, with the offset due to camber at zero angle of attack very well predicted and the variation with angle of attack not as well predicted. At the higher Mach number, the incremental moment due to camber is almost constant, while the increment at the smaller Mach number is non-linear, especially for the largest nose deflection.

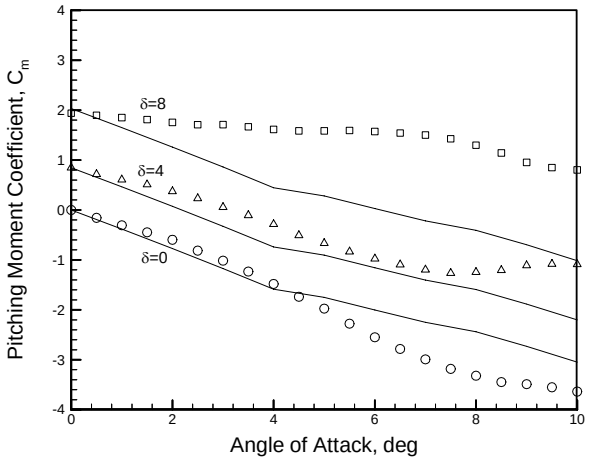

Fig. 21. Effect of Nose Deflection on Pitching Moment Mach=3, AIAA 2003-3805

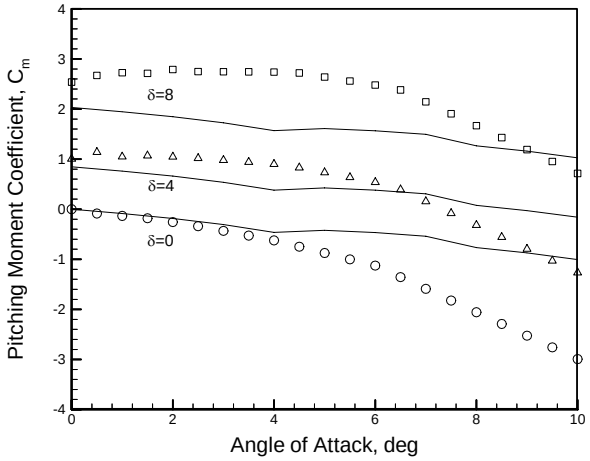

Fig. 22. Effect of Nose Deflection on Pitching Moment Mach=6, AIAA 2003-3805

Additional Modifications

The axial force due to inlets or fins that are not symmetrically arranged around the body also contribute to pitching moment at zero angle of attack. Although the inlet contribution was already calculated in Missile Datcom, the fin contribution was not, so this has been added (Subroutines SYTNHS).

IV Conclusion

A method for analyzing cambered bodies has been incorporated into Missile Datcom. Two existing methods were evaluated, one based on slender body theory and one based on mean line theory. The addition of a contribution due to viscous crossflow improved the predictions for both methods. The methods were compared against wind tunnel data from subsonic to supersonic speeds for cambered bodies with axi-symmetric cross-sections. Comparison cases consisted of three configurations with discrete camber changes (deflectable nose missiles) and eleven configurations with continuous camber changes. The combination of slender body theory with a viscous crossflow contribution was found to compare more accurately with experimental data and was incorporated into Missile Datcom.

References

1. Blake, W.B., "Missile Datcom User's Manual – 5/97 Fortran 90 Revision," AFRL-VA-WP-TR-1998-3009, February 1998.

2. Packard, J.D., and Miller, M.S., "Assessment of Engineering Level Codes for Missile Aerodynamic Design and Analysis," AIAA paper 2000-4590, presented at the Atmospheric Flight Mechanics Conference, Denver CO, August 2000.

3. Sooy, T.J., and Schmidt, R.Z., "Aerodynamic Predictions, Comparisons, and Validations Using Missile Datcom (97) and AeroPrediction 98 (AP98)," AIAA paper 2004-1246, presented at the Aerospace Sciences Meeting, Reno NV, January 2004.

4. Stevenson, M.D., Zweber, J.V., Bhungalia, A.A., Moster, G.E., Grandhi, R.V., and Forest, M.P., "Multi-Disciplinary Conceptual Vehicle Modeling," AIAA paper 2001-1430, presented at the AIAA Structures, Structural Dynamics and Materials Conference, Seattle WA, April; 2001.

5. Riley, D.R., "Some Effects of Nose Deflection and Number of Tail Fins on the Aerodynamic Characteristics in Pitch and Sideslip of a Wingless Missile At a Mach Number of 3.11," NASA TM X-270, April 1960.

6. Williams, J.E., Jr., and Vukelich, S.R., "The USAF Stability and Control Digital Datcom – Volume II, Implementation of Datcom Methods," AFFDL-TR-79-3032, April 1979.

7. Bennett, B.K., "Conceptual Design Synthesis Tool for Arbitrary-Body Missiles," AIAA paper 97-2281, presented at the Applied Aerodynamics Conference, Atlanta GA, June 1997.

8. Keuthe, A.M., and Schetzer, J.D., Foundations of Aerodynamics, John Wiley & Sons, New York, 1961.

9. Liepmann and Roshko, Elements of Gasdynamics, John Wiley and Sons, New York, 1957.

10. Beane, B., and Durkin, F.; "The Effects of Body Camber on Body Pressure Distributions and Wing Forces for M=2 to 7.6," ASD TR 61-295, March 1962.

11. Nielsen, J.N., Missile Aerodynamics, McGraw Hill. New York, 1960.

12. Allen, H.J., "Estimation of the Forces and Moments Acting on Inclined Bodies of Revolution of High Fineness Ratio," NACA RM A9I26, November 1949.

13. Gapcynski, J.P., "The Effect of Camber on the Aerodynamic Characteristics of a Body at a Mach Number of 2.01," NASA TM X-56, September 1959.

14. Spencer, B., Jr., Phillips, W.P., and Fournier, R.H., "Supersonic Aerodynamic Characteristics of a Series of Bodies Having Variations in Fineness Ratio and Cross-Section Ellipticity," NASA TN D-2389, August 1964.

15. Phillips, W.P., and Spencer, B., Jr., "Transonic Aerodynamic Characteristics of a Series of Bodies Having Variations in Fineness Ratio and Cross-Section Ellipticity," NASA TN D-2622, February 1965.

16. Shrout, B.L, and Covell, P.F., "Aerodynamic Characteristics of a Series of Bodies with Variations in Nose Camber," NASA TP 2206, September 1983.

17. Horton, A., and McDaniel, M., "Correction of Axial Force Prediction Discrepancies due to AoA in Missile Datcom," AIAA paper 2005-4833, Applied Aerodynamics Conference, Toronto, Canada, June 2005.

18. Landers, M.G., Hall, L.H., Auman, L.M., and Vaughn, M.E., Jr, "Deflectable Nose and Canard Controls for a Fin-Stabilized Projectile at Supersonic and Hypersonic Speeds," AIAA paper 2003-3805, Applied Aerodynamics Conference, Orlando, FL, June 2003.